CEBAF Program Advisory Committee Eight Cover Sheet

This proposal must be received by close of business on Thursday, April 14, 1994 at:

CEBAF
User Liaison Office, Mail Stop 12 B
12000 Jefferson Avenue
Newport News, VA 23606

Proposal Title

Measurement of small components of the ^{3}He wave function using $^3\overrightarrow{\mathrm{He}}$ ($\vec{e}$,e'p) in Hall A

Contact Person

F. W. Hersman
University of New Hampshire
Department of Physics
Durham, NH 03824
Office: (603)868-6362 FAX: (603) 868-2998
email: hersman@unh.edu

Experimental Hall:	Hall A
Total Days Requested for Approval:	24 days
Minimum and Maximum Beam Energies (GeV):	1.6 GeV → 4.0 GeV
Minimum and Maximum Beam Currents (μAmps):	25 μA

CEBAF Use Only

Receipt Date: 4/14/94 PR 94-023

By: [illegible]

HAZARD IDENTIFICATION CHECKLIST

CEBAF Experiment: 94-023 Date: 5/26/94

Check all items for which there is an anticipated need—do not check items that are part of the CEBAF standard experiment (HRSE, HRSH, CLAS, HMS, SOS in standard configurations).

Cryogenics ____ beamline magnets ____ analysis magnets ____ target ____ drift chambers ____ other	**Electrical Equipment** ____ cryo/electrical devices ____ capacitor banks ____ high voltage ____ exposed equipment	**Radioactive/Hazardous Materials** List any radioactive or hazadorous/ toxic materials planned for use: ____ ____
Pressure Vessels ✓ 0.5 cm inside diameter 10 bar operating pressure glass window material 20 μm window thickness	**Flammable Gas or Liquids** (incl. target) type: ____ flow rate: ____ capacity: ____	**Other Target Materials** ___ Beryllium (Be) ___ Lithium (Li) ___ Mercury (Hg) ___ Lead (Pb) ___ Tungsten (W) ___ Uranium (U) ___ Other (list below) ____ ____
Vacuum Vessels ____ inside diameter ____ operating pressure ____ window material ____ window thickness	**Radioactive Sources** ____ permanent installation ____ temporary use type: ____ strength: ____	**Large Mech. Structure/System** ____ lifting devices ____ motion controllers ____ scaffolding or elevated platforms ____ other
Lasers type: Ar^+ | Ti:Saph wattage: 30 | 6 class: ____ | ____ **Installation** ____ permanent ✓ temporary **Use** ____ calibration ____ alignment	**Hazardous Materials** ____ cyanide plating materials ____ scintillation oil (from) ____ PCBs ____ methane ____ TMAE ____ TEA ____ photographic developers ____ other (list below) ____ ____ ____	**Notes:** ____ ____ ____ ____ ____ ____

A NEW PROPOSAL TO THE 6/94 CEBAF PAC

Measurement of small components of the ^{3}He wave function using $^3\overrightarrow{He}$ ($\vec{e}$,e'p) in Hall A

F. W. Hersman, L. C. Balling, V. Boykin, J. Calarco,
J. Distelbrink, L. Gelinas, J. Heisenberg, M. Kennedy,
V. Pomeroy, Timothy P. Smith, I. The, A. Tutein, J. Wright
University of New Hampshire

M. B. Leuschner
Indiana University

B. Wojtsekhowski
RPI

R. Lourie, S. vanVerst
University of Virginia

currently seeking the endorsement of the Hall A Collaboration

F. W. Hersman, contact person

ABSTRACT

We propose to measure polarization observables of $^3\overrightarrow{He}$($\vec{e}$,e'p) in the quasielastic region to extract information on the small components of the helium wave function. We exploit the high resolution capability of the HRS spectrometers to separate two-body (d), quasi-two-body (d*), and three-body (pn) final states. The high density target is based on existing techniques for polarizing helium by alkali spin exchange. Parallel kinematics are chosen with constant kinetic energy of 350 MeV in the final state (CM) system to minimize final state interaction effects and make them uniform for all kinematics. Two beam-target asymmetries in the scattering plane, A'_x and A'_z, and the normal asymmetry A^0_y are all measured for the three final missing energy ranges. Statistical uncertainties in the physical asymmetries better than 0.01 over the range of missing momentum from $0 < p_m < 400$ MeV/c in 100 MeV/c bins are obtained in 24 days.

In addition to the unique physics provided by separating states in final missing energy, Hall A offers greater experimental systematic and statistical precision as well. The high luminosity in Hall A (relative to Hall B) provides the majority of events at optimal angles relative to the fixed target direction. Furthermore, since the (e,e'p) reaction is kinematically focussed, greater statistical precision is obtained in higher luminosity, fixed aperture spectrometers. Studies of the kinematics using Monte Carlo simulations are presented in Chapter 4 with the final estimates of the uncertainty.

2. Structure of ^{3}He and related asymmetries

In their paper on spin dependent electron scattering from polarized ^{3}He, Blankleider and Woloshyn[3] discuss the momentum distributions of both neutrons and protons relative to the spin of the nucleus. They use the solutions to the Fadeev equations[4] obtained by Afnan and Birrell. They present a partial wave decomposition of the structure in the Derrick-Blatt scheme. In particular, $L-S$ coupling is used, and the spin-isospin states are combined to make states of definite symmetry under the interchange of two particles. The probabilities of the partial wave channels appear in Table 1.

Channel number	L	S	l_α	L_α	P	K	Probability (%)
1	0	0.5	0	0	A	1	87.44
2	0	0.5	0	0	M	2	0.74
3	0	0.5	1	1	M	1	0.74
4	0	0.5	2	2	A	1	1.20
5	0	0.5	2	2	M	2	0.06
6	1	0.5	1	1	M	1	0.01
7	1	0.5	2	2	A	1	0.01
8	1	0.5	2	2	M	2	0.01
9	1	1.5	1	1	M	1	0.01
10	1	1.5	2	2	M	2	0.01
11	2	1.5	0	2	M	2	1.08
12	2	1.5	1	1	M	1	2.63
13	2	1.5	1	3	M	1	1.05
14	2	1.5	2	0	M	2	3.06
15	2	1.5	2	2	M	2	0.18
16	2	1.5	3	1	M	1	0.37

Table 1. The partial wave channels of the ^{3}He wave function.

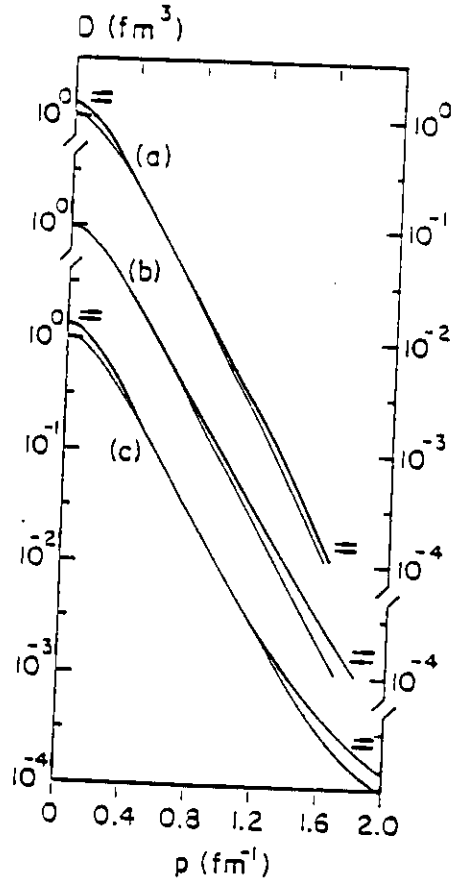

Fig. 1. The proton spin-dependent momentum distribution for a fixed azimuthal angle $\xi = 45°$. Curves correspond to a proton with its spin parallel and antiparallel to the spin of ^{3}He. In a) only the S- and S′-state are included, in b) the S- and D-state are included, and in c) the S-, S′-, and D-states are included.

They explore the sensitivity of the small components of the ^{3}He wave function by examining the momentum distribution with individual partial waves selected. The dominant components, channels 1 and 4 are totally antisymmetric in spin-isospin (and symmetric in space) and therefore contribute nothing to spin dependent scattering. They observed that only two components, channel 2, the S′-state, and channel 11, the D-state, have significant spin dependence in their momentum distributions. (Fig. 1)

Laget has calculated the quasielastic scattering $^3\overline{\mathrm{He}}(\bar{e},e'p)$ reaction at various kinematics and target angles. He objective was to explore the non-vanishing asymmetries A'_x, A'_z, and A^0_y, and determine their sensitivity to ingredients in the wave-function and

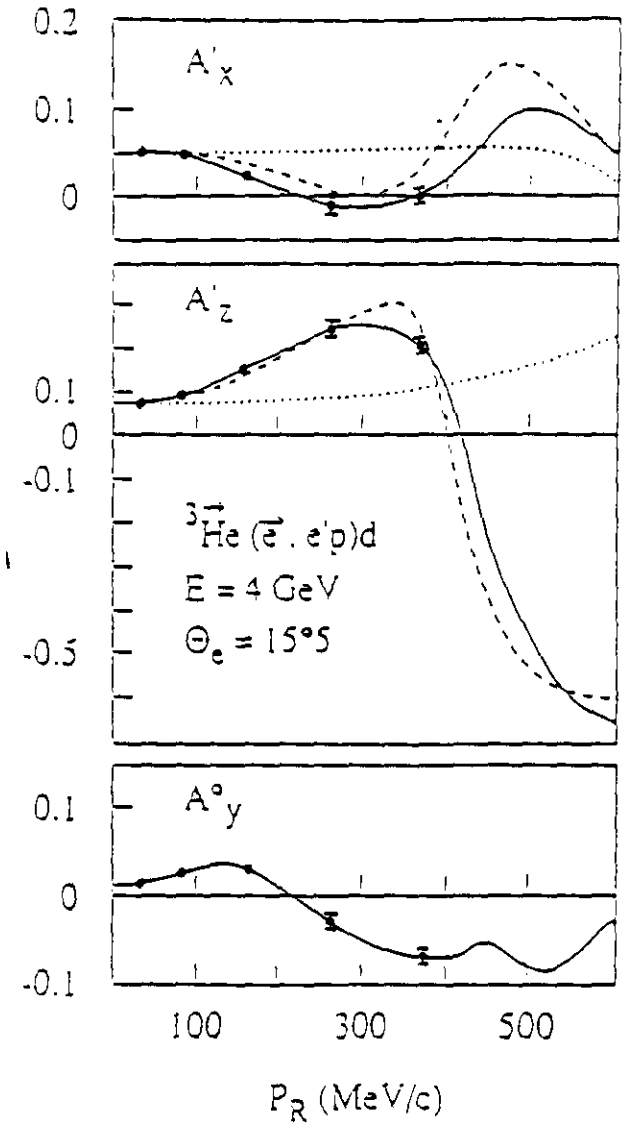

Fig. 2. The three target asymmetries which do not vanish in collinear kinematics are plotted against the momentum p_R of the deuteron recoiling in the reaction $^3\vec{He}(\vec{e},e'p)d$. The incoming electron energy is 4 GeV. The dotted lines and dashed lines correspond to PWIA when only the S-wave or both the S- and D-wave are respectively taken into account. The full lines include FSI and MEC. The data points indicate the kinematics and projected uncertainties of the present proposal.

reaction dynamics. Of particular interest is whether wave function information can be extracted unambiguously from the polarization observables.

Calculations were performed in parallel kinematics and high momentum transfer to minimize the effects of final state interactions. Reactions leading to the two body final

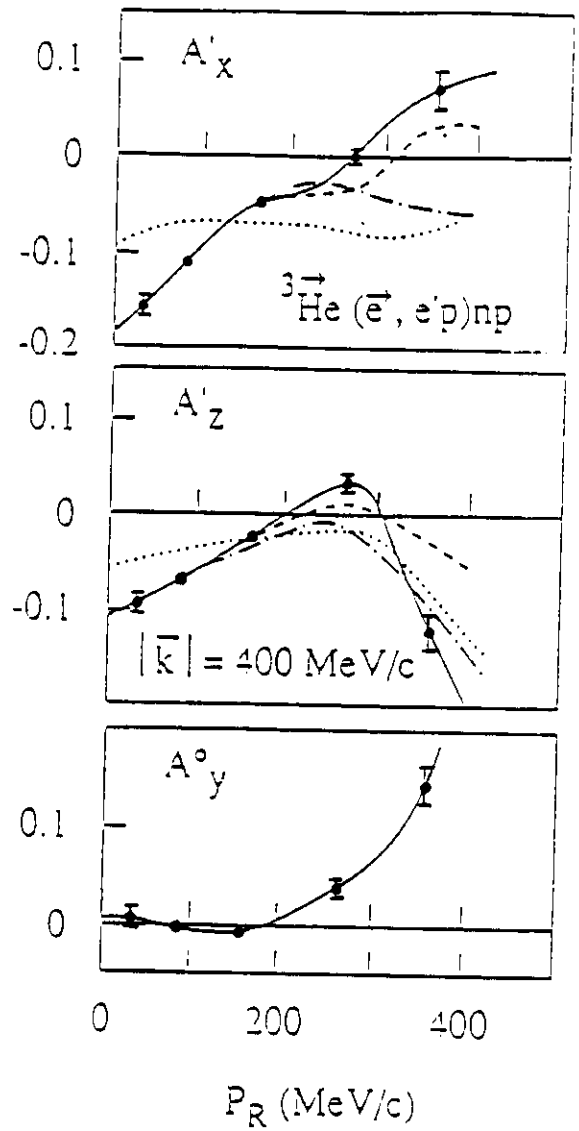

Fig. 3. The three target asymmetries which do not vanish in collinear kinematics are plotted against the average value of the momentum of the pn pair recoiling in the reaction $^3\overrightarrow{He}(\vec{e},e'p)pn$. (Fig. 2) The incoming electron energy is 0.8 GeV. The dotted lines, the dash-dotted lines, and the dashed lines correspond to PWIA when only the S-wave, the S-wave and S'-wave, and the S-, S'-, and D-wave are respectively taken into account. The full lines also include FSI and MEC. The uncertainties indicated on the projected data represent the *larger* of the d^* or integrated continuum three-body breakup regions.

state (Fig. 2) and to the three-body continuum (Fig. 3) were studied. (Calculations to the quasi-two-body d^* final state are yet available.) The sensitivity of these calculations on the small components in the structure was explored by including different choices of partial waves. Plane wave results and results including FSI and MEC were provided for comparison.

3. Experimental Details

3.1 Target

The target technology we have selected for this measurement has been developed over the past 8-10 years by the Princeton group.[5] and used in several measurements at several laboratories. The high density and high polarization offered by this technology provides an excellent figure of merit for studies where maximum density is important. It has already been used very successfully for a deep inelastic scattering measurement at SLAC that had target requirements similar to ours. Furthermore, refinements of this technology continue to offer improvements in performance. It is appropriate to mention that an alternative technology is being pursued at Mainz in which helium nuclei are polarized by metastability exchange and compressed. This technology has also provided excellent performance and offers further improvements as well. We discuss below our plans in terms of the SLAC spin exchange target parameters, and outline briefly our program for improvements.

We will use a ^{3}He target pressurized to 10 atmospheres of helium, or $2.7\times10^{20}/\mathrm{cm}^3$ over a length of 15 cm. for a total thickness of $4\times10^{21}/\mathrm{cm}^2$ or 20 mg/cm^2. A beam current of 25 μA (1.5×10^{14}) will provide a luminosity of 6×10^{35} electron-^{3}He/cm^{2}sec. The extended target acceptance of the HRS of 10 cm allows all of the target to be viewed at the relevant scattering angles between 12° and 15°. A longer target is being considered. A new concave inward design for the window[6] has been developed at UNH and tested at 5 atmospheres without beam. In-beam tests are planned at Bates. It may be kept in mind that if beam related failures of the glass window under high pressure becomes a concern, the target cell may be placed in an environment pressurized to 10 atmospheres without substantial difficulty.

The ^{3}He target is polarized by optically pumping an alkali metal vapor (rubidium) which spin exchanges with helium. Circularly polarized light of 795 nm (the D_1 line) is absorbed by s-shell electrons with the opposite spin, promoting them to the $p_{1/2}$-shell. Subsequent collisions with helium and nitrogen mix the p-shell polarization and promote nonradiative decays to the ground state, with equal probability for each spin state. The depletion of one spin state leads to accumulation of rubidium atomic polarization. Polarization is transferred to helium nuclei through the hyperfine interaction during collisions.

The design uses two cells, a pumping cell and a target cell. The pumping cell is maintained at elevated temperature, adjusted to control the rubidium vapor pressure. It is located 5 cm off-axis and at an angle of 45° with respect to the beam. It must

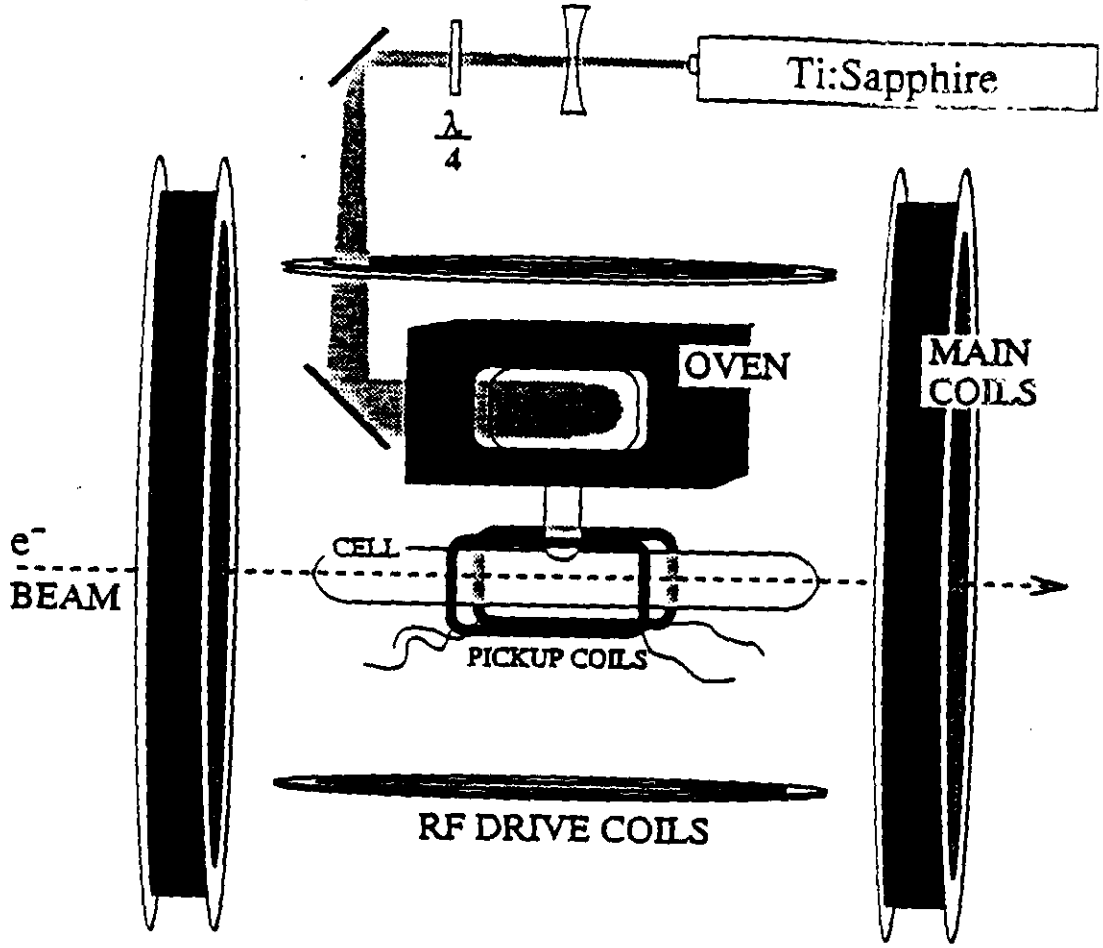

Fig. 4. The SLAC E142 alkali spin exchange helium target.[7,8] The target design we propose differs only in the cell diameters and the window design.

be fully illuminated to maximize the polarization. The target cell is held at a lower temperature to assure that the rubidium plates out on the transfer tube and does not enter the target cell. (Fig. 4) Target polarization is measured by adiabatic fast passage nuclear magnetic resonance. An integrated measure of beam polarization times neutron polarization is extracted from one of the scattering asymmetries.

Coincidence quasielastic scattering from neutrons in 100 torr of nitrogen contributes a 14% dilution over the volume of the cell. Coincidences from scattering off of neutrons in the glass windows can be eliminated by electron track reconstruction. Scattering from nitrogen is measured with an equivalent target of the same geometry (with additional nitrogen) and subtracted. While remaining uncertainties in this dilution contribute to uncertainties in the cross section, they do not contribute to uncertainties in the extracted ratio of electric to magnetic form factor. We continue seeking design possibilities that reduce the nitrogen thickness.

The largest source of rubidium depolarization is wall contact, which must be overcome with laser intensity. We intend to maximize the polarization by reducing the diameter of the pumping cell, minimizing the surface area and concentrating the laser power. A simple analysis indicates that significantly higher rubidium densities can be pumped at fixed laser power, leading to substantially faster polarization rates. While we use the parameters of the SLAC target for our estimates, we intend to develop a target with pumping cell and target cell diameters of 5 mm. First prototype tests are underway.

3.2 Magnetic fields

The quantization axis is provided by a set of Helmholtz coils. The diameter is chosen as large as possible to provide a maximally uniform field, while maintaining clearance from the quadrupoles Q1 in the forward position at 90 cm. We choose a radius of 60 cm. A slightly larger Helmholtz pair is oriented perpendicular to the first. This coil set will be used for slow polarization rotation and reversal, and also for providing the quantization axis during adiabatic fast passage nuclear magnetic resonance (the polarization will be measured in a different orientation than the data taking to simplify the pickup coil design).

The magnetic field from Q1 in the vicinity of the target reaches a maximum on order of 1 gauss. We intend to suppress stray magnetic fields from the quadrupoles Q1 using a field clamp. We are planning to study the effectiveness of a "doughnut" shaped iron plate mounted 15 cm from the quadrupole aperture in providing a return path for stray flux. If necessary a similar sheet of mu-metal will be added a short distance in front of the plate.

The angle of the momentum transfer direction is different for the five measurements, ranging from $-51.03°$ at the lowest missing momentum to $-27.79°$ at the highest missing momentum. The parallel asymmetry is measured with the quantization axis along the momentum transfer. The perpendicular asymmetry requires target axis ranging from $38.97°$ to $62.21°$. Since the glassware requires a single photon polarization axis (chosen at $45°$), a small (few percent) loss of polarization will be due to this misalignment. The target can be rotated about the beam axis and the laser redirected to provide the perpendicular quantization axis. The normal asymmetries are measured with a separate target cell.

Magnetic fields associated with the beam current are of little significance to depolarization since the repetition rate is far from resonance with the Larmor precession of the nuclei.

3.3 Beam polarization

A high current high polarization photocathode will be used for this experiment, providing 75% beam polarization. Condensed matter researchers at New Hampshire are preparing to contribute to the development and fabrication of reliable high efficiency photocathodes. Beam polarization will be measured by Møller polarimetry, to a precision of approximately 3%. This uncertainty does not contribute significantly to the final result.

4. Plan for measurement of quasielastic asymmetries

We describe our plans to measure quasielastic asymmetries in $^3\overrightarrow{\mathrm{He}}(\vec{e},e'p)$ to determine the structure of small components in the ^{3}He wave function. Three asymmetries are separately measured. The two in plane asymmetries are measured by selecting different target angles, such that the momentum transfer direction is either parallel or perpendicular to the quantization axis. Finally the normal target asymmetry A_y^0 is measured separately, providing a calibration of the final state interactions and meson exchange currents.

4.1 Kinematics

Kinematics are selected to cover the range of missing momentum from $0 < p_m < 400$ MeV/c. Each kinematics is chosen such that the kinetic energy in the final state is constant, in our case 350 MeV. The fact that it is constant makes the largest source of uncontrolled ambiguity, final state interactions, apply the same to each kinematics. Comparisons with theory are further simplified since only one continuum calculation is required. The value chosen, 350 MeV, is located at a minimum in the energy dependent nucleon-nucleon interaction, minimizing the magnitude of the FSI. The central missing energy was chosen as 50 MeV to more efficiently use the acceptance of the spectrometers. Finally the beam energy is chosen to be the maximum for which the momentum transfer can be reached with the minimum scattering angle of 12.6°. Kinematics are tabulated in Table 1.

TABLE 1

Kinematics for asymmetry measurements

	E_0	Q^2	$\vec{q}$	ω	$\theta_{e'}$	θ_q	p	p_m
A	4.0	0.962	1.152	0.604	15.30	-51.03	1.152	0.000
B	4.0	0.664	0.984	0.551	12.60	-49.86	1.080	0.095
C	3.2	0.415	0.820	0.507	12.60	-45.77	1.011	0.191
D	2.4	0.223	0.668	0.473	12.60	-39.00	0.948	0.280
E	1.6	0.089	0.539	0.449	12.60	-27.79	0.896	0.357

Count rate estimates were performed with the Monte Carlo reaction code MCEEP. The nominal HRS acceptance in the electron arm of $\delta\theta = \pm 32$ mr and $\delta\phi = \pm 72$ mr was assumed, with momentum acceptance of $\delta p = \pm 5\%$. For the proton acceptance the forward quad mode for the HRS spectrometer was used, with $\delta\theta = \pm 36$ mr and $\delta\phi = \pm 93$ mr, and momentum acceptance of $\delta p = \pm 4\%$. The two body breakup reaction process was modeled using the momentum distribution measured by Jans[9] and Marchand[10] for generation of events in the spectrometer acceptances. The spectral function of Meier-Hajduk[11] was used to generate three body breakup events. Two missing energy regions were defined in the three body breakup channel: the d* corresponding to $5.5 < E_m < 12.5$ MeV, and the continuum with $E_m > 12.5$ MeV. Rates for the five kinematics in each of these missing energy regions are reported in Table 2.

TABLE 2

Rates into the full acceptances (sec^{-1})

	p_m range	d	d*	pn
A	0 → 65	13.7	5.57	0.87
B	45 → 125	20.2	10.1	2.60
C	105 → 225	9.60	7.81	4.22
D	205 → 325	1.23	1.28	2.19
E	305 → 430	0.24	0.09	0.66

TABLE 3

. Uncertainties in physical asymmetries: $\Delta A = (p_e\ p_{^3He}\sqrt{N})^{-1}$ and

	$\Delta A(d)$	$\Delta A(d^*)$	$\Delta A(pn)$	hours
A	0.0030	0.0048	0.012	24×3
B	0.0025	0.0036	0.0070	24×3
C	0.0036	0.0040	0.0055	24×3
D	0.010	0.010	0.0076	24×3
E	0.013	0.022	0.0080	72×3

Uncertainties in the physical asymmetries are calculated from the total counts and the beam and target polarization by

$$\Delta A = (p_e\ p_{^3He}\sqrt{N})^{-1}.$$

Beam polarization of 75%, and target polarization of 40% were used in the calculations. For the run times indicated in Table 3, an extracted precision on the asymmetries of better than 1% can be obtained for most kinematics. (Better statistics is requested for the high count rate kinematics to explore cuts on the data, and systematic effects.) Anticipated data for two body breakup are plotted in Figure 2, against a calculation by Laget in similar (antiparallel) kinematics. In Figure 3 the larger of the uncertainties of the three body breakup regions is plotted next to a calculation of significantly different kinematics. Nevertheless the sensitivity of these asymmetries to the small components of the structure and the ability of the measurement to determine the asymmetries is apparent. We request a total of 21 days of beam time to measure three asymmetries to three final state missing energy regions at five choices of missing momentum kinematics. Three days target change time and background subtraction is added to bring the total request to 24 days.

4.2 Institutional Commitment

The University of New Hampshire group has had for many years an MOU to design and implement the Hall A trigger for the two HRS spectrometers. John Calarco is leading that effort. The design work is now complete, and the first batch of electronics is being purchased. The UNH group also has a collaborative effort with the UNH Atomic Physics group to fabricate a polarized target for an approved experiment at the Saskatchewan Accelerator Laboratory. We intend to provide a similar target for these measurements.

1. Bates experiment 89-12. J.F.J. van den Brand and R. G. Milner, spokesme (1990).

2. CEBAF Proposal 91-020. R. McKeown, spokesman.

3. B. Blankleider and R. M. Woloshyn, *Phys. Rev.* **C29** (1984) 538.

4. I. R. Afnan and N. D. Birrell, *Phys. Rev.* **C16** (1977) 823.

5. T. E. Chupp, *et al.*, *Phys. Rev.* **C45** (1992) 915 and references therein.

6. F. W. Hersman, Proceedings of the Conference on Polarized Ion Sources and Polarized Gas Targets, Madison, WI (1993)

7. H. Middleton, *et al.*, Proceedings of the Conference on Polarized Ion Sources and Polarized Gas Targets, Madison, WI (1993)

8. G. D. Cates, Polarized Targets in High Energy Physics, preprint.

9. E. Jans, *et al.*, *Phys. Rev. Lett.* **49** (1982) 974.

10. C. Marchand, *et al.*, *Phys. Rev. Lett.* **60** (1988) 1703.

11. H. Meier-Hajduk, *et al.*, *Nucl. Phys.* **A395** (1983) 332.